

## Structure of Nylon 46 Lamellar Crystals: An Investigation Including Adjacent Chain Folding

Salvador León, Carlos Alemán, Marta Bermúdez, and Sebastián Muñoz-Guerra\*

Departament d'Enginyeria Química, Universitat Politècnica de Catalunya, ETSEIB, Diagonal 647, 08028 Barcelona, Spain

Received July 13, 2000; Revised Manuscript Received September 20, 2000

**ABSTRACT:** The structure of nylon 46 lamellar crystals was investigated by molecular dynamics simulations taking into account the occurrence of chain folding. Fold arrangements compatible with adjacent chain reentry were simulated and comparatively analyzed. The  $C_{14}$  fold consisting of a 14-membered loop with one amide group included in the fold was found to be the most stable arrangement. Computer simulation of crystal models including the folds revealed that the packing preferences of the nylon in the lamellar crystals were not altered by changes in the chain-folding mechanism. Results confirmed the energy similitude between the  $\alpha$  and  $\beta$  forms of nylon 46 and supported the occurrence of a statistical lattice composed of these two forms as the most probable structure for nylon 46 chain-folded crystals. Monte Carlo simulations were also carried out to confirm the suitability of such statistical structure and to account for certain thermal effects observed by experimentation.

### Introduction

Nylon 46 is a polyamide of AA–BB type made from tetramethylenediamine and adipic acid, which was first synthesized by Carothers,<sup>1</sup> and that is marketed nowadays by DSM under the name Stanyl. The crystal structure of this nylon, both in the bulk and in lamellar crystals grown from solution, has been investigated by a number of authors.<sup>2–4</sup> All of them coincide in reporting a structure made of hydrogen-bonded sheets with chains in fully extended conformation, but they do not agree either on the manner in which the chains are hydrogen bonded within the sheets or on which pattern is followed for the stacking of the sheets.

Very recently, we have investigated the structure and morphology of nylon 46 crystals grown from solution by combining electron microscopy and X-ray diffraction data with energy calculations and molecular modeling.<sup>5</sup> The more noticeable features of such crystals are illustrated in Figure 1. They are rectangular lamellae consisting of twinned structure with the hydrogen-bonded sheets running parallel to the long dimension of the crystal and with chains standing normal to the lamellar surface. The energy analysis favored a crystal lattice in which hydrogen bonds are aligned perpendicular to the chain axis (normal scheme) and sheets are progressively shifted along the  $c$ -axis (called  $\beta$  form by analogy to the  $\beta$  form of nylon 6<sup>6</sup>). The same model but with the sheets shearing up and down along the  $c$ -axis (called  $\alpha$  form for its similitude with the  $\alpha$  form of nylon 6<sup>6</sup>) was found to entail an energy penalty of only 0.5 kcal mol<sup>-1</sup> residue<sup>-1</sup>. On the contrary, those other models with hydrogen bonds set in an oblique scheme, i.e., running at 77° to the chain axis like in nylon 66,<sup>7</sup> appeared to be much less stable (Figure 2). A mixed lattice composed of normally hydrogen-bonded sheets arranged in a statistical array of  $\alpha$  and  $\beta$  forms with a  $\Delta c$  displacement of either 2.33 or 3.66 main chain bonds was concluded to be the most appropriate to represent the structure of nylon 46 in lamellar crystals.

The same lattice was found to be also valid to describe the structure of the cocrystals made from an equimolar mixture of nylon 46 and nylon 5.<sup>8,9</sup>

The thickness of nylon 46 lamellae grown from solution is about 7.5 nm whereas the calculated molecular length of the polymer was over 100 nm when the chain is arranged in fully extended conformation. Molecules must fold up-and-down at the surface of the lamellae and therefore to be able to reenter into the crystalline core. In fact, ordered decorating patterns indicative of regular sharp chain folding have been observed for certain preparations of nylon 46 crystals after shadowing with polyethylene vapors according to Wittmann and Lotz.<sup>10</sup> Chain folding and sheet packing are closely related features which should be considered together for an integrate description of chain-folded lamellar crystals. In the case of nylon 46 lamellae, a detailed examination of the folds appears to be specially advisable because (i) a chain folding mechanism containing one amide group, a feature that distinguishes nylon 46 from other higher nylons and approaches it to poly( $\alpha$ -amino acid)s, has been postulated<sup>4</sup> and (ii) the energy implied in the fold could outweigh the relative stability of the different crystal forms and change therefore the structural preferences inferred on the exclusive basis of packing considerations.

Despite the relevance that chain folding may have to the crystal structure of nylon 46, little attention was paid to this matter in previous studies. In this work we wish to report on the structure and morphology of nylon 46 lamellar crystals taking into account the presence of reentrant chain folding. The study has been carried out using molecular dynamics (MD) simulations to model the folding mechanism for the two types of sheet stacking ( $\alpha$  and  $\beta$ ) present in nylon 46 lamellae and for the most stable  $\Delta c$  displacements. In the first place the relative stability of the fold as a function of the nature and size of the loop was examined. Then the influence of the folding mechanism on the crystal structure was evaluated. Finally, Monte Carlo (MC) simulations were used to reexamine the statistical model proposed in our previous work,<sup>5</sup> and theoretical results were correlated

\* Corresponding author: E-mail: munoz@eq.upc.es.

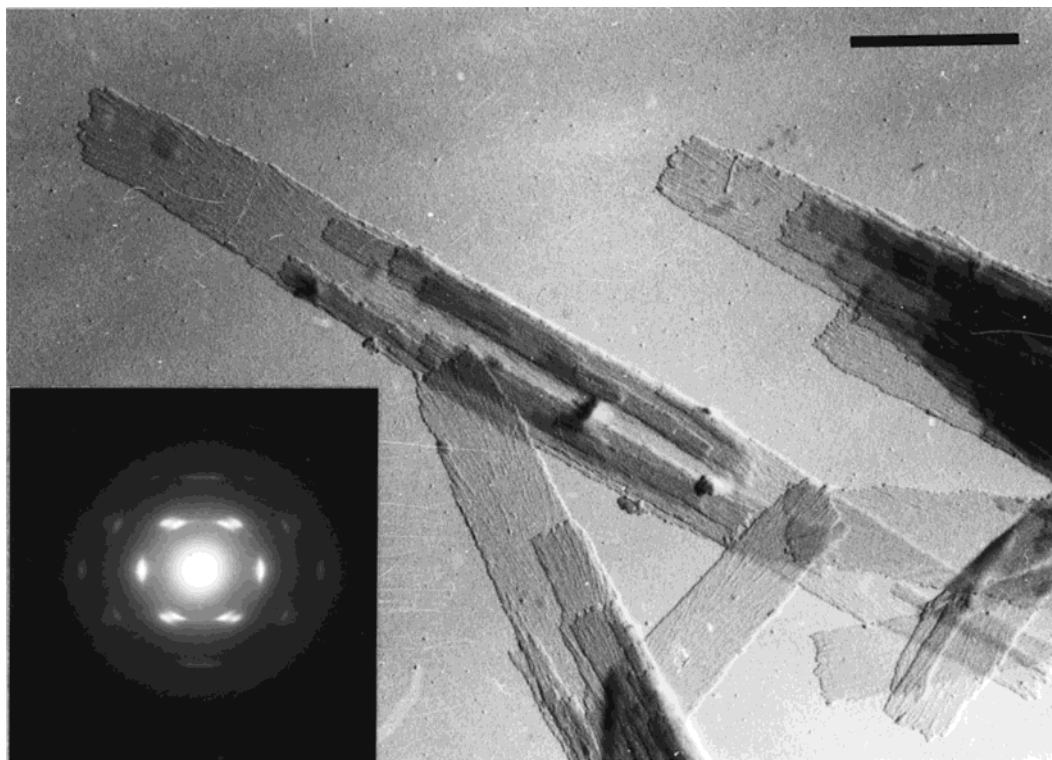


**Figure 1.** Bright-field electron micrograph of nylon 46 lamellar crystals grown from glycerin at 177 °C and shadowed with Pt–C. The scale bar stands for 1  $\mu\text{m}$ . Inset: electron diffraction pattern produced by such crystals and inserted in the corresponding relative orientation.

with certain significant observations provided by crystallization and annealing experiments. For a comprehensive understanding of this work, a careful reading of the previous paper,<sup>5</sup> in which the structure of nylon 46 crystals disregarding chain folding was investigated throughout, is strongly advised.

## Methods

**Experimental Methods.** Nylon 46 used in this work was kindly supplied by Dr. Eltink of DSM. The received sample was fractionated by precipitation from a formic acid solution using ethanol as precipitant. The fraction selected for this study had an intrinsic viscosity in dichloroacetic acid of 0.9 dL g<sup>-1</sup>, which, according to the viscosity equation established for nylon 66,<sup>11</sup> corresponds to a molecular weight of about 18 000.

Single crystals of nylon 46 were obtained by crystallization from dilute solution in glycerin or 1,4-butanediol at temperatures of 130 or 177 °C, respectively. They were then collected by centrifugation and repeatedly washed with butanol. The electron and X-ray diffraction analysis of these crystals was reported in detail in previous works.<sup>5,9</sup> For crystal surface examination, crystals deposited on grids were decorated with polyethylene vapors and then shadowed with Pt–C according to the method developed by Wittmann and Lotz.<sup>10</sup> The annealing treatment was applied to nylon 46 crystals deposited on the electron microscopy grids used for observation. A Philips EM-301 electron microscope operating at 80 or 100 kV was used in this study.

**Computational Procedure.** MD simulations were performed with the Amber 3.0 computer package.<sup>12</sup> The strategy adopted in this work consists of three different levels of application, along which the complexity of the system was progressively increased. First, all the possible folds involved in adjacent chain folding were simulated using a small model molecule in order to compare the relative stability of the respective conformations. Next, the energy of the most stable folds was examined considering a whole sheet of hydrogen-bonded chains. Finally, a set of stacked hydrogen-bonded

sheets was used to mimic the chain-folded lamellar crystal. To increase the computational efficiency, the coordinates of the residues that are not involved in the folding mechanism were frozen in all the simulations by using the BELL option of the Amber program.<sup>12</sup> MD simulations were carried out at 298 K, using a 2 fs time step, and coordinates were saved every 1000 fs for further analysis steps. Prior to the MD simulations, the energy of the system was minimized to a gradient of 0.1 kcal mol<sup>-1</sup> nm<sup>-1</sup>.

The effect of the temperature on the crystal structure of nylon 46 was investigated using Monte Carlo (MC) simulations, which were performed using a parallelized version of the MCDP (Monte Carlo for Dense Polymers) computer program.<sup>13</sup> For the present study, the Metropolis algorithm<sup>14,15</sup> was chosen among the different strategies implemented in MCDP. The large efficiency of the MCDP program to investigate the crystal structure of polyamides has been recently proved.<sup>16</sup> The models subjected to study consisted of 22 independent sheets, each one made of two nylon 46 stems containing six repeating units and arranged in antiparallel. Both alternating ( $\alpha$ ) and progressive ( $\beta$ ) shearing models were considered for the stacking of the sheets. Such a large number of sheets was taken in order to ensure a good representation for the statistical model proposed for nylon 46.<sup>5</sup> NVT simulations were performed at  $T = 298$  K and  $T = 503$  K considering both periodic continuation conditions and the minimum-image convention. The nonbonded interactions were truncated at 1 nm. The degrees of freedom in the simulations were the setting angle of each chain and the amount of shearing between successive sheets.

The PCSP (Prediction of Crystal Structure of Polymers) computer program<sup>17</sup> was used to generate the atomic coordinates of the investigated models. This program was specifically developed to build and analyze three-dimensional arrangements of polymers fitted in a crystal lattice. MD simulations were run in a Silicon Graphics R-10000 at our laboratory. MC simulations were performed in a Origin 2000 Silicon Graphics with 64 MIPS processors at the Centre Europeu de Paral·lelisme de Barcelona (CEPBA).

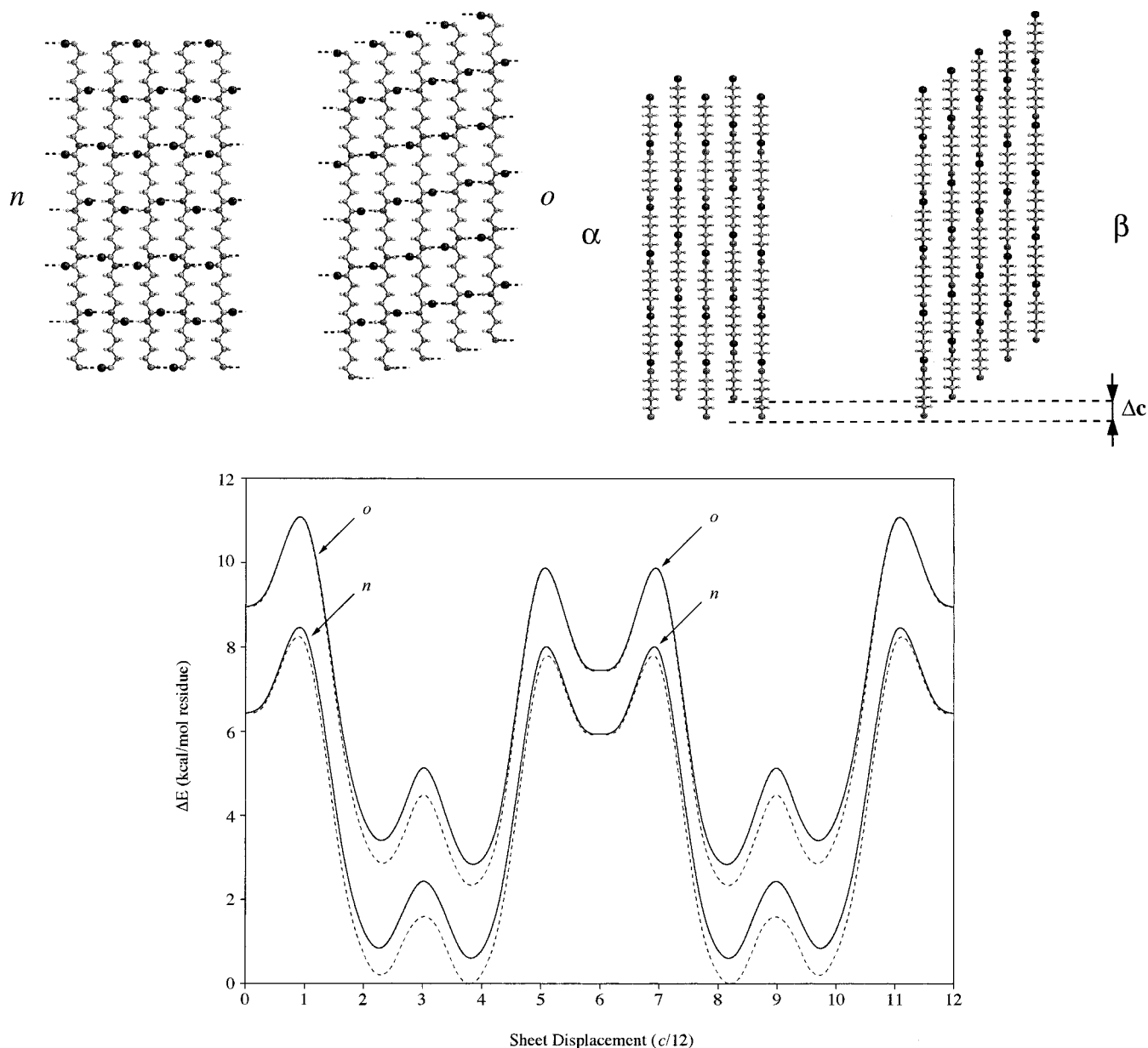


**Figure 2.** (upper) Two hydrogen-bonding schemes (normal, *n*, and oblique, *o*) feasible for fully extended nylon 46 chains within the hydrogen-bonded sheets and the two models for the stacking of the sheets along the *c*-axis (alternating,  $\alpha$ , and progressive,  $\beta$ ). (lower) Relative energy vs  $\Delta c$  displacement for the  $\alpha$ - and  $\beta$  forms (solid and dashed lines, respectively) with hydrogen bonds set in either the normal (*n*) or the oblique (*o*) scheme. The shift of the sheets along the *a*-axis is progressive in all cases.

## Results and Discussion

**Electron Microscopy Observations.** As is illustrated in Figure 3, decoration of nylon 46 lamellar crystals with polyethylene vapors afforded more or less regular decorating patterns depending on the thermal history of the sample. No sign of ordering was detected for crystals grown in glycerin at 177 °C (Figure 3a), in spite that nucleation on the lamellar surface has been effective as the small size of the decorating rods reveals. On the contrary, nylon 46 crystals grown at 130 °C in 1,4-butanediol provided fairly regular decorating patterns with the polyethylene particles showing a preferential orientation normal to the long axis of the crystal (Figure 3b), an observation that had been already reported by Atkins et al.<sup>4</sup> This type of pattern is taken as indicative of the occurrence of chain folding planes parallel to the large lateral faces of the crystals. We have obtained the same result when 1,4-butanediol was replaced by glycerin, indicating that the solvent is not

determinant of such an effect. Electron diffraction showed that the *c*-projected structure is essentially the same for all solution-grown crystals whatever are the conditions used for crystallization.<sup>5</sup> On the other hand, significant effects on the lamellar surface of nylon 46 crystals were observed when they were subjected to annealing. Thus, crystals shown in Figure 3c, which were grown in glycerin at 177 °C and then heated at 230 °C for 30 min, display partially ordered decorating patterns with the polyethylene rods frequently aligned as in Figure 3b. X-ray diffraction taken from mats of these crystals indicated that a partial conversion of the  $\alpha$  form into the  $\beta$  form seems to take place upon heating.<sup>5</sup> The relevant conclusion drawn from these results is that both low temperatures of crystallization and annealing treatment promote an increase of ordering on the surface of nylon 46 lamellar crystals.

**Modeling of the Chain Folds.** The four different folding mechanisms that may be conceived for the



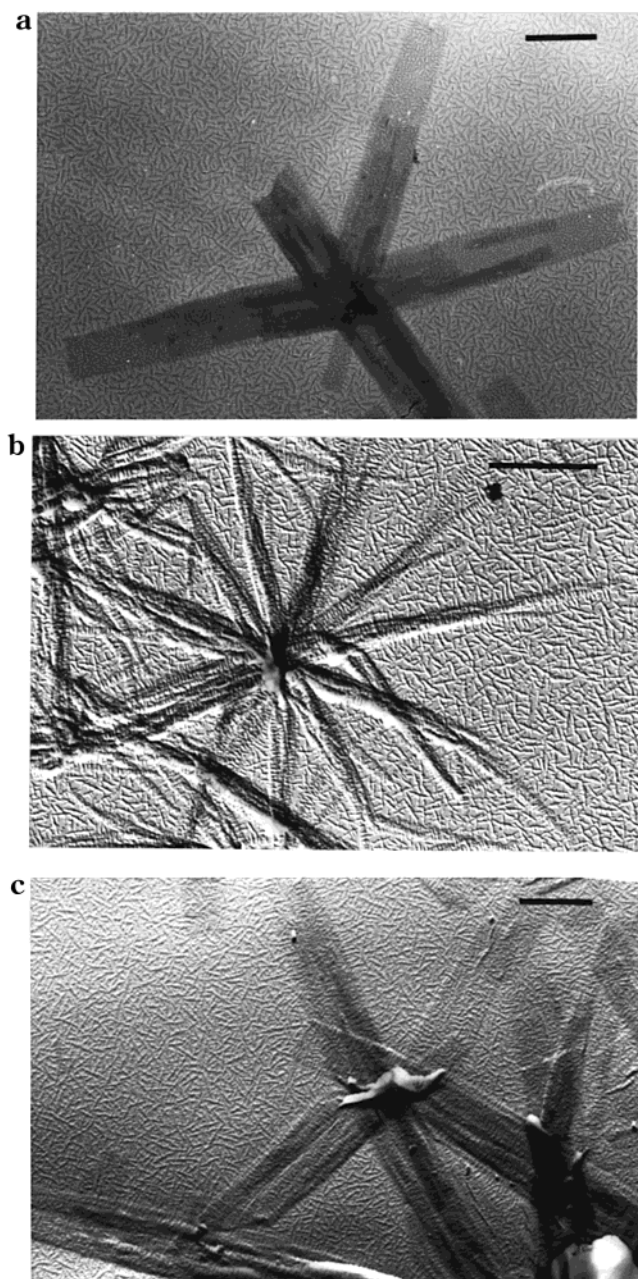


**Figure 3.** Nylon 46 lamellar crystal grown from glycerin solution and surface-decorated with vapor-deposited polyethylene: (a) crystals grown at 177 °C; (b) crystals grown from 1,4-butanediol at 130 °C; (c) crystals grown at 177 °C and subjected to annealing at 230 °C for 30 min. The scale bar represents 1  $\mu\text{m}$  in the three cases.

adjacent reentry of a nylon 46 chain in a hydrogen-bonded sheet are depicted in Figure 4. If hydrogen bonds are set perpendicular to the chain axis, two folds, both of them incorporating one amide group in the loop, are feasible. These folds are denoted as  $C_{14}$  and  $C_{16}$ , respectively, according to the number of atoms contained in the hydrogen-bonded ring that composes the fold. Another two folds are feasible in the case that hydrogen bonds in the sheets are arranged in an oblique scheme. These are denoted as  $C_{9C}$  and  $C_{9N}$ , indicating that both of them contain nine atoms in the hydrogen-bonded loop and that the chain moiety involved in the fold is the diacid tetramethylene or the diamine hexamethylene segment, respectively.

The four folds were simulated considering a model molecule consisting of five chemical residues of nylon

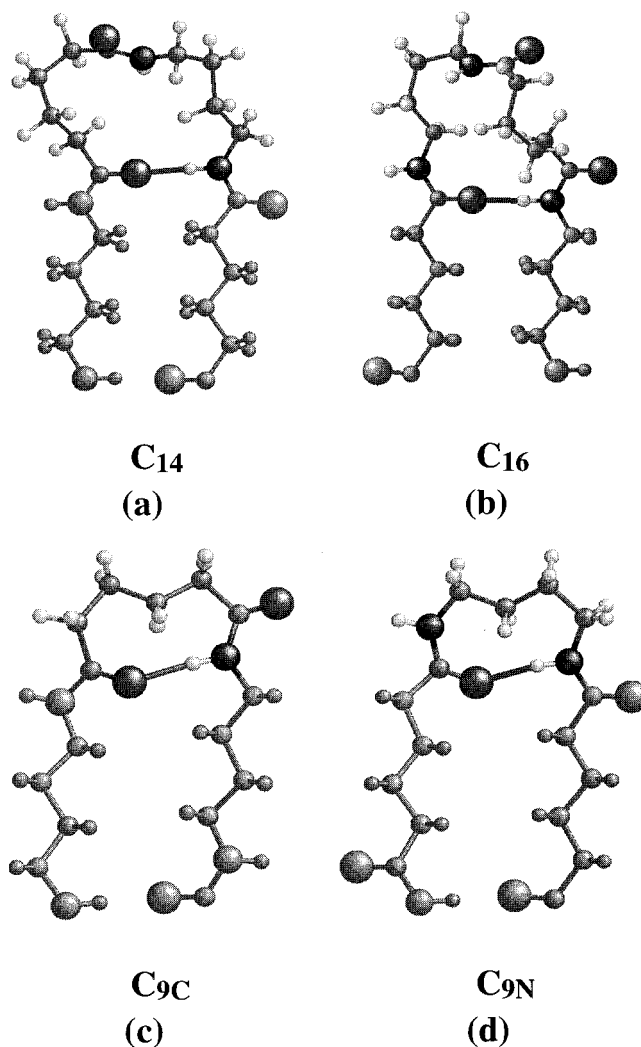


**Figure 4.** Feasible folds for adjacent reentry nylon 46 chain. (a)  $C_{14}$ : 14-membered hydrogen-bonded ring containing one amide group in the fold. (b)  $C_{16}$ : 16-membered hydrogen-bonded ring containing one amide group in the fold. (c)  $C_{9C}$ : nine-membered hydrogen-bonded ring involving the diacid alkane segment in the fold. (d)  $C_{9N}$ , nine-membered hydrogen-bonded ring involving the diamine alkane segment in the fold.

46. The fold was built using the central residue, and the hydrogen bonds set between the amide groups of the remaining residues were restrained to equilibrium values according to the hydrogen-bonding scheme (normal or oblique) adopted in each case. The MD simulations were run for a total of 1000 ps. The overall energies of the folds are compared in Figure 5 as a function of the simulation time. The energy is referred to one chemical residue providing a reliable picture of the relative stability of the four folding arrangements possible for nylon 46. The energy traces show that folds associated with chains hydrogen-bonded according to the oblique scheme ( $C_{9N}$  and  $C_{9C}$ ) are much less stable than those others occurring in chains with hydrogen bonds in the normal scheme ( $C_{14}$  and  $C_{16}$ ) and that destabilization is maximum when the diamine segment is included in the fold. They show also that the  $C_{14}$  fold is favored with respect to the  $C_{16}$  fold in only about 5  $\text{kcal mol}^{-1}$  residue $^{-1}$ . Since such a small difference could be canceled out by energy differences due to the stacking of the sheets, it seems advisable to evaluate the influence of packing effects on the relative stability of the folds. This will be done in the next section for the three

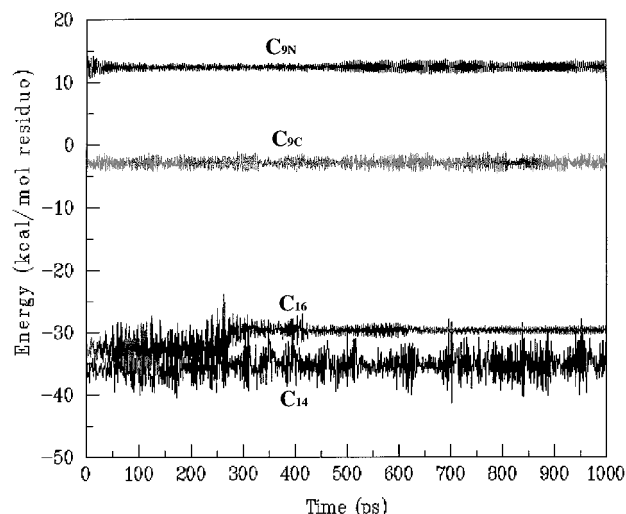


**Figure 5.** Energy of the  $C_{14}$ ,  $C_{16}$ ,  $C_{9C}$ , and  $C_{9N}$  folds as a function of the simulation time. The energy is referred to one chemical residue for the  $C_{14}$  and  $C_{16}$  folds and to a half of chemical residue for the  $C_{9C}$  and  $C_{9N}$  ones.

lower energy folds; since the  $C_{9N}$  fold is particularly unstable, it will be ignored in the following simulations in order to save computational costs.

**Chain-Folded Crystals.** Adjacent chain-folded sheets were built using the PCSP computer program for the three most favored folding arrangements, i.e., for the  $C_{14}$ ,  $C_{16}$ , and  $C_{9C}$  folds. Each sheet was built from a single nylon 46 chain containing 48 chemical residues. The chain was folded up-and-down every six residues to conform the lamellar height experimentally measured for nylon 46 crystallized from solution.<sup>5</sup> At this stage, intrasheet chain effects were evaluated by running MD simulations for the three models restraining the hydrogen bonds within the sheet. No significant variations in the relative stability of the different models obtained in the analysis of the individual folds were detected. In view of these results, we proceeded with the simulation of the whole crystal using a set of stacked hydrogen-bonded sheets. The systems that have been analyzed with expression of the parameters of the respective unit cells are described in Table 1.

**The  $\beta$  Form.** In our previous works it was found that the  $\beta$  form with a displacement of 3.66 main chain bonds along the  $c$ -axis is the most stable structure for nylon 46 lamellar crystals.<sup>5,9</sup> Accordingly, we have used this structure to build the folded crystal models for energy

analysis. These models were made of five sheets with chains folded according to the  $C_{14}$ ,  $C_{16}$ , and  $C_{9C}$  arrangements. The evolution of the potential energy for the central sheet, considering both intra- and intermolecular contributions, along the MD simulations is displayed in Figure 6a for the three chain-folded crystal models.

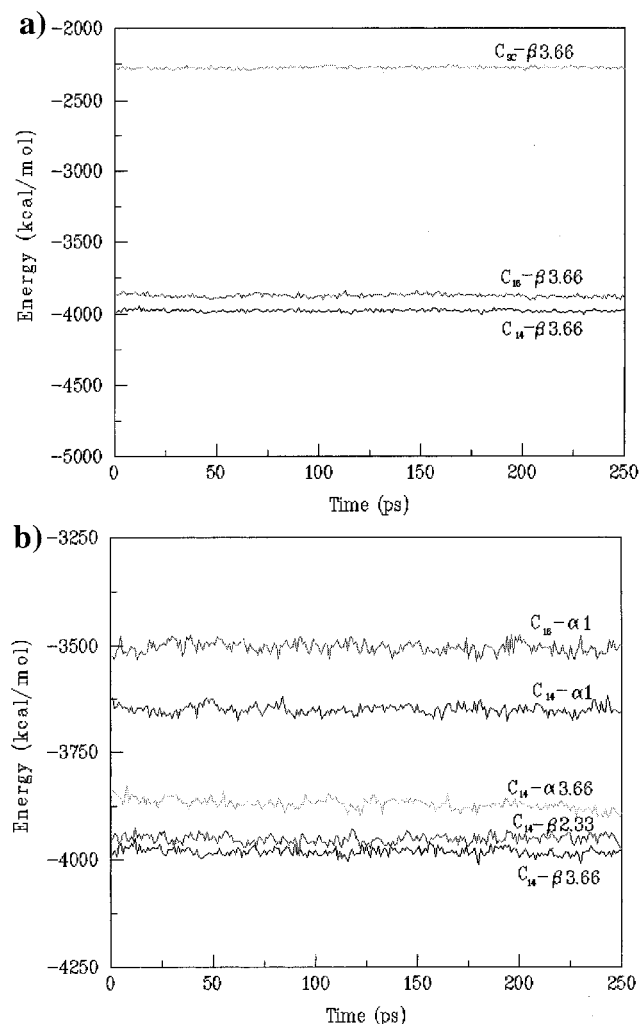
MD calculations revealed that the crystal made of  $C_{9C}$  folds continues to be much less stable than those built with  $C_{14}$  and  $C_{16}$  folds. It was revealed also that the former presents unfavorable interactions between the tetramethylene segment of the fold elements belonging to adjacent sheets. Such destabilizing interactions cannot be minimized because the conformation of the loop in the  $C_{9C}$  fold is severely restricted. On the other hand, the crystal containing the  $C_{14}$  fold continues to be slightly more stable than that consisting of  $C_{16}$  folds. Although the amide groups may be hydrogen bonded to each other in both types of fold, these interactions were found to take place more easily for the  $C_{14}$  fold. Thus, an analysis of the snapshots stored along the simulation runs revealed that the amount of formed hydrogen bonds was about 68% and 48% of the complete theoretical number for the crystals with chain folded according to  $C_{14}$  and  $C_{16}$  folds, respectively. It should be mentioned that in all the simulations hydrogen bonds present a dynamical behavior, being continuously broken and remade along the trajectories. For illustration purposes, the  $C_{14}$ - $\beta$ 3.66 chain-folded structure resulting after 250 ps of MD trajectory is displayed in Figure 7.

A very interesting point concerning the stability of the crystal forms of nylon 46 is the energy difference between the models with  $\Delta c$  displacements of 3.66 and 2.33 main chain atoms. Molecular mechanics calculations indicated that these minimum-energy arrangements are almost isoenergetic, the latter being less favored than the former by about 0.1 kcal mol<sup>-1</sup> residue<sup>-1</sup> (Figure 2b). To see how chain folding may affect the relative stability of these two minima, additional MD simulations of a lamellar crystal in the  $\beta$  form with  $\Delta c = 2.33$  were performed considering the  $C_{14}$  fold ( $C_{14}$ - $\beta$ 2.33). As can be seen in Figure 6b, the energy resulting from such simulation almost matches that obtained for the  $\beta$  form with a displacement of 3.66 main chain bonds with the same fold. These results indicate that chain folding does not change the relative stability of these closest packing models and that therefore conclusions previously reached do not need to be revised.

**Table 1. Chain-Folded Crystal Models Examined in This Work**

crystal lattice							
sheet stacking scheme <sup>a</sup>	H-bonding scheme <sup>a</sup>	$\Delta c$ displacement <sup>b</sup>	unit cell <sup>c</sup> $a, b, c$ (nm) $\alpha, \beta, \gamma$ (deg)	reference	folding	chain-folded crystal model	
$\beta$	$n$	3.66	0.965, 0.613, 1.470	5	$C_{14}$	$C_{14}$ - $\beta$ 3.66	
			42.9, 90.0, 107.2		$C_{16}$	$C_{16}$ - $\beta$ 3.66	
		2.33	0.965, 0.505, 1.470	5	$C_{9C}$	$C_{9C}$ - $\beta$ 3.66	
			55.5, 90.0, 110.8		$C_{14}$	$C_{14}$ - $\beta$ 2.33	
$\alpha$	$n$	3.66	0.965, 0.826, 1.470	this work	$C_{14}$	$C_{14}$ - $\alpha$ 3.66	
		1.00	90, 90, 115		$C_{14}$	$C_{14}$ - $\alpha$ 1	
			0.965, 0.826, 1.470		$C_{16}$	$C_{16}$ - $\alpha$ 1	

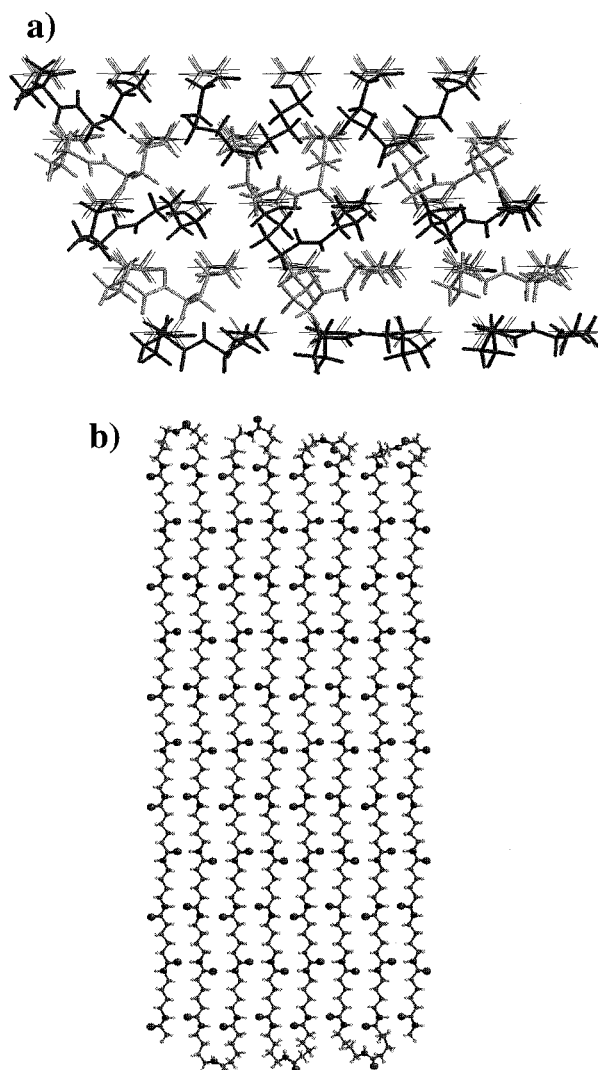
<sup>a</sup> Schemes for the stacking of the sheets and for the hydrogen bonds within the sheets, as illustrated in Figure 2a. <sup>b</sup> Sheet displacement between successive sheets expressed as the number of main chain bonds. <sup>c</sup> Unit cells parameters according to the molecular arrangement; note that geometry differences arise from the differences in the mode in which sheets are stacked but the projected unit cell down the  $c$ -axis is the same for all the structures.



**Figure 6.** Energy of the lamellar nylon 46 chain-folded crystals as a function of the simulation time for the indicated folds arrangements. In all cases the energy is referred to the central chain-folded sheet. (a) The three crystal models were built considering a  $\beta$  form with a displacement of 3.66 main chain bonds along the  $c$ -axis. (b) Crystal models corresponding to  $\alpha$  and  $\beta$  forms at the indicated displacements and involving the indicated fold arrangements.

To have a deeper insight into the  $C_{14}$  folded structure, the torsional angles corresponding to the 11 freely turntable bonds contained in the loop were statistically analyzed. The results for each torsional angle are shown in Table 2, where conformations have been grouped in six population categories: *cis*, *gauche*<sup>+</sup>, *skew*<sup>+</sup>, *trans*, *gauche*<sup>-</sup>, and *skew*<sup>-</sup>. As can be seen, the *trans* is the preferred conformer, revealing that a small fraction of torsional angles are involved in the construction of the loop. More specifically, the *trans* conformation leaves to be the most populated one only in the torsion associated with 4, 7, 8, and 11 bonds.

**Comparison with the  $\alpha$  Form.** In our previous works, it was found that the  $\alpha$  form of nylon 46 is about 0.5 kcal mol<sup>-1</sup> residue<sup>-1</sup> less stable than the  $\beta$  form and that both forms share an energy minimum for a  $\Delta c$  displacement of 3.66 main chain atoms.<sup>5,9</sup> To investigate the effect of chain folding on the relative stability of the  $\alpha$  and  $\beta$  forms, we have carried out a comparative study of these two forms with chains folded according to the  $C_{14}$  arrangement. We have also included in this study the model proposed by Atkins et al. for the lamellar crystals of nylon 46.<sup>4</sup> This model is described as an  $\alpha$

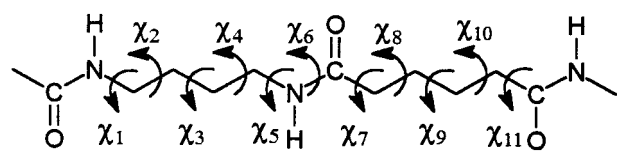


**Figure 7.** Details of the chain-folded structure proposed for the lamellar crystal of nylon 46: (a) fold surface as it is seen with the crystal projected down the  $c$ -axis (the  $C_{14}$  folds and the chain stems are represented in black and gray, respectively); (b) hydrogen-bonded sheet with  $C_{14}$  folds as viewed along the  $b$ -axis of the crystal.

form with hydrogen-bonded sheets displaced one main chain bond along the  $c$ -axis. Accordingly, three additional molecular models in the  $\alpha$  form, one of them with  $\Delta c = 3.66$  ( $C_{14}$ - $\alpha 3.66$ ) and the other two with  $\Delta c = 1.0$  ( $C_{14}$ - $\alpha 1$ ,  $C_{16}$ - $\alpha 1$ ) were simulated by MD. The energy trajectories resulting for these models and referred to the central sheet are compared in Figure 6b with those obtained for the  $\beta$  form in the previous section by similar calculations. As can be seen, the  $\beta$  form continues to be the more stable one, showing that the influence of chain folding on the relative stability of the packing modes is not significant. This makes sense since the number of interactions arising from the packing of the sheets throughout the whole crystal is much larger than those associated with possible contacts among neighboring folding loops.

The same conclusions could be drawn when the energies of the  $\alpha 1$  models were comparatively evaluated. Our previous studies<sup>5</sup> have revealed that nylon 46 crystal models with sheets displaced in  $\pm 1$  main chain atom entail energy excesses from 1.5 up to more than 5 kcal mol<sup>-1</sup> residue<sup>-1</sup>, depending on the specific arrangement that is adopted. As is seen in Figure 6b, this mode



**Table 2. Conformational Distribution of the Torsional Angles Contained in the C<sub>14</sub> Fold of Nylon 46 Lamellar Crystals<sup>a</sup>**


	<i>cis</i>	<i>gauche</i> <sup>+</sup>	<i>skew</i> <sup>+</sup>	<i>trans</i>	<i>skew</i> <sup>-</sup>	<i>gauche</i> <sup>-</sup>
$\chi_1$	0	0	1	81	18	0
$\chi_2$	0	34	8	54	2	2
$\chi_3$	0	1	2	96	1	0
$\chi_4$	2	91	1	0	0	6
$\chi_5$	0	10	26	46	18	0
$\chi_6$	0	0	1	98	1	0
$\chi_7$	1	15	15	0	37	32
$\chi_8$	0	73	2	2	3	20
$\chi_9$	0	2	3	87	4	4
$\chi_{10}$	0	3	6	74	5	12
$\chi_{11}$	0	10	51	39	0	0

<sup>a</sup> The population analysis (in %) of the 11 torsional angles ( $\chi_i$ ) is specified.

of packing continues to be relatively unstable after including chain folding in the crystal model. In other words, the poor stability of the  $\alpha$ 1 models produced by an unfavorable  $\Delta c$  cannot be altered by the chain folding mechanism. An additional point that is worthy of mention is that the C<sub>14</sub>- $\alpha$ 1 model appears to be more stable than the C<sub>16</sub>- $\alpha$ 1 one, in agreement with the conclusions reached in previous sections for the models in the  $\beta$  form.

To evaluate the energy contribution of the folding to the energy of the system, the energies given in the profiles displayed in Figure 6a were decomposed into the contributions associated with the sheets and the folds. Results revealed that the energy order among the different folds is the same in the simulations of an isolated fold than in those inserted in a crystal. However, energy differences are considerably smaller in the latter case. Accordingly, the C<sub>16</sub> and C<sub>9C</sub> folds were 0.1 and 3.8 kcal mol<sup>-1</sup> residue<sup>-1</sup> less stable than the C<sub>14</sub> fold, respectively, when the crystal environment was considered. These results indicate that a comprehensive description of the environment is required to evaluate the influence of the chain folding on the crystal structure of nylons and that simulations of isolated systems may lead to an overestimation of the energy differences.

A second factor contributing to the relative stabilization of the  $\beta$  form concerns hydrogen bonding among amide groups contained in the folds. As a consequence of the recuperative shearing characteristic of the  $\alpha$  form, the amide group included in the C<sub>14</sub> fold can be hydrogen bonded to only one out of their two neighboring amide groups (Figure 8a). MD simulations revealed that the second hydrogen bond cannot be formed even when the loops were considerably distorted. This means that the maximum amount of hydrogen bonds that can be formed in the fold surface of a lamellar crystal in the  $\alpha$  form is only 50% of the theoretically total number. Conversely, all the amide groups may be comfortably hydrogen-bonded to their two neighboring groups in a model with sheets progressively stacked, as it occurs in the  $\beta$  form (Figure 8b).

**Statistical Model of Nylon 46 and the  $\alpha$ -to- $\beta$  Conversion.** Nylon 46 crystals grown in glycerin (Figure 1) at 177 °C have been described as a statistical

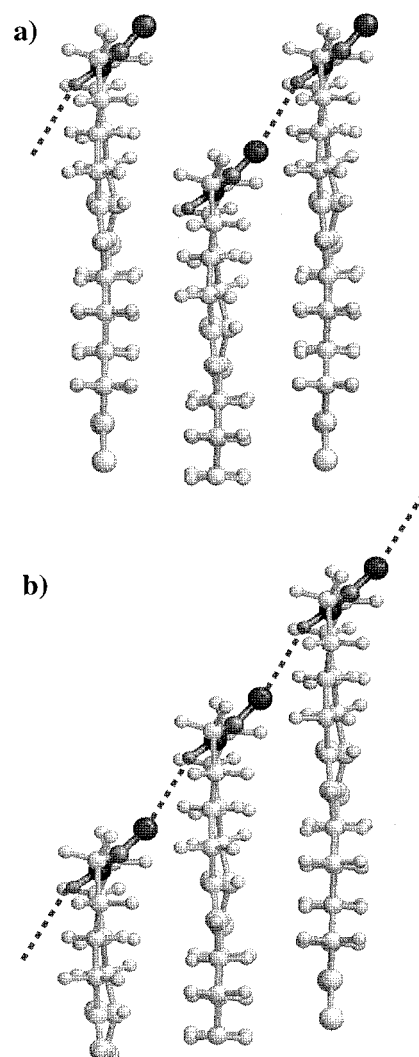


**Figure 8.** Hydrogen bonds between the amide groups included in the C<sub>14</sub> folds: (a) the  $\alpha$  form and (b) the  $\beta$  form. It should be noticed that in the  $\alpha$  form the amide group can participate in only one hydrogen bond whereas in the  $\beta$  form two hydrogen bonds are possible for each amide group.

lattice of  $\alpha$  and  $\beta$  forms with successive sheets displaced along the *c*-axis by either 2.33 or 3.66 main chain atoms. The lack of surface regularity displayed by these crystals after polyethylene decoration (Figure 3a) is taken as a manifestation of the wavy nature of the basal lamellar plane caused by the uneven stacking of the chain-folded sheets. The regular decorating pattern displayed by the same crystals after annealing is associated with a partial  $\alpha$ -to- $\beta$  conversion induced by the thermal treatment. To substantiate these interpretations, we have carried out MC molecular simulations taken into account the effect of the temperature on the statistical structure. The analysis has been performed on an infinite crystal of nylon 46 by applying periodic boundary conditions along the three axis. For this purpose, 22 independent sheets, each one composed of two nylon 46 stems in antiparallel arrangement, were packed in either the  $\alpha$ - or the  $\beta$  form with a displacement of 3.66 main chain bonds in both cases ( $\alpha$ -3.66 and  $\beta$ -3.66). These models were used as the starting geometry for MC simulations carried out at  $T = 298$  K and  $T = 503$  K. Chain folding was not included in these simulations since it was previously concluded that its influence on the crystal structure may be neglected.

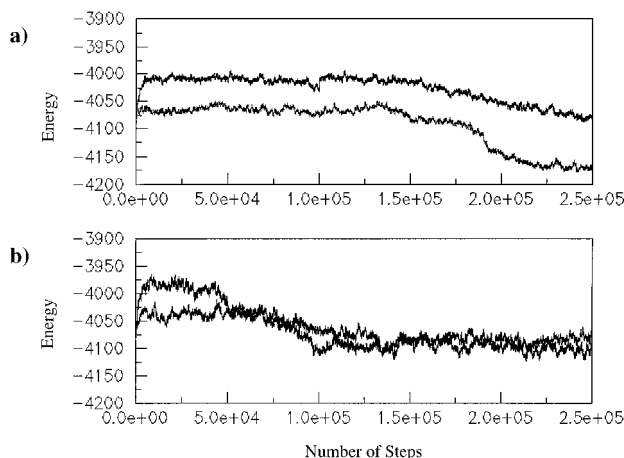


**Figure 9.** Energy of crystal models for nylon 46 as a function of the number of MC steps for simulations at  $T = 298$  K (a) and  $T = 503$  K (b). The dark and gray lines correspond to the  $\alpha$  and  $\beta$  forms, respectively. Initially both structures were built with a sheet displacement of 3.66 main chain bonds along the  $c$ -axis.

Figure 9a displays the energies of the complete system at 298 K provided by MC calculations. It is worth noting that the  $\beta$ -3.66 model is more stable than the  $\alpha$ -3.66 one by about  $75 \text{ kcal mol}^{-1}$ , in agreement with our previous molecular mechanics calculations.<sup>5</sup> Such difference in energy was found to almost vanished when simulations were performed at 503 K, a temperature similar to that applied in the annealing treatment (Figure 9b). The conclusion from this result is that conversion from  $\alpha$  to  $\beta$  must be governed by kinetic factors; the statistically mixed structure that is formed by crystallization in solution becomes enriched in  $\beta$  form upon annealing because the energy required to jump is provided by such treatment.

The evolution of  $\Delta c$  along the course of the simulation process revealed a spontaneous tendency of the sheets in the  $\beta$  form initially shifted by 3.66 main chain atoms to be displaced at  $\Delta c = 2.33$ . This is illustrated in Figure 10 where the  $\Delta c$  displacement is represented as a function of the number of steps. It is worth noting that the change in the sheet displacement took place after a few steps of simulation and that the number of changing sheets increased with temperature. The same behavior was observed in the simulation of a crystal of nylon 46 initially built in the  $\alpha$  form although in such case  $\Delta c$  displacements were widely dispersed within the 3.66–2.33 range. These results are in accordance with energy predictions made by molecular mechanics calculations (Figure 2b) and corroborate the preference of nylon 46 for a statistical structures essentially composed of sheets sheared at 3.66 and 2.33 main chain atoms. It should be remarked that the occurrence of such a statistical lattice simplifies the description of the crystal structure of nylon 46 since differences between  $\alpha$  and  $\beta$  forms almost disappear. Comparison of Figure 10 with Figure 9a reveals that increasing the statistics of the lattice with regards to the  $\Delta c$  displacements adds stability to the structure, regardless of whether the initial sheet arrangement was alternating or progressive. Thus, the energy of the two models decreased by 80–100  $\text{kcal mol}^{-1}$  after about  $2.0 \times 10^5$  steps, a point of the

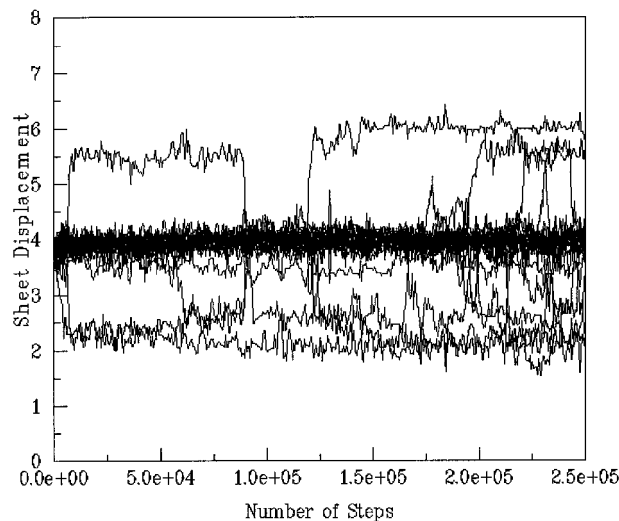


**Figure 10.** Variation of the shear of the sheets in the  $c$  direction in the  $\beta$  form along the MC simulations at  $T = 298$  K. The starting structures was built with a displacement of the sheets along the  $c$ -axis of 3.66 main chain bonds.

simulation process where a significant fraction of sheets have abandoned their initial shearing displacements.

**Acknowledgment.** The authors thank Dr. S. J. E. A. Eltink for kindly supplying the nylon 46 sample and to DGCYT for financial support (Grant PB-96-0490). They are also indebted to the European Center of Parallelism at Barcelona (CEPBA) for computational facilities. Salvador León acknowledges the grant given by the Ministerio de Educación y Cultura to support the realization of his Ph.D.

## References and Notes

- (1) Carothers, W. H. U.S. Patent 2, **1938**, 130, 948.
- (2) Gaymans, J.; Doeksen, D. K.; Harkema, S. In *Integration of Fundamental Polymer Science and Technology*; Kleintjens, P., Lemstra, L., Eds.; Elsevier Pub.: Amsterdam, 1985; p 573.
- (3) Kashima, M.; Kusanagi, H.; Ishimoto, A. *Polym. Prepr., Jpn.* **1991**, 40, E1488.
- (4) Atkins, E. D. T.; Hill, M.; Hong, S. K.; Keller, A.; Organ, S. *Macromolecules* **1992**, 25, 917.
- (5) Bermúdez, M.; León, S.; Alemán, C.; Muñoz-Guerra, S. *J. Polym. Sci., Polym. Phys.* **2000**, 38, 41.
- (6) Holmes, D. R.; Bunn, C. W.; Smith, D. J. *J. Polym. Sci.* **1955**, 17, 159.
- (7) Bunn, C. W.; Garner, E. V. *Proc. R. Soc. London* **1947**, A189, 39.
- (8) Bermúdez, M.; León, S.; Alemán, C.; Muñoz-Guerra, S. *Polym. Prepr., ACS* **1999**, 81, 244.
- (9) Bermúdez, M.; León, S.; Alemán, C.; Muñoz-Guerra, S. *Polymer* **2000**, 41, 8961.
- (10) Wittmann, J. C.; Lotz, B. *J. Polym. Sci., Polym. Phys. Ed.* **1985**, 23, 205.
- (11) Elias, W. H.; Shumacher, R. *Makromol. Chem.* **1964**, 76, 23.
- (12) Singh, U. C.; Weiner, P. K.; Cadwell, J.; Kollman, P. *AMBER 3.0*. Rev. A, University of California.
- (13) León, S.; Alemán, C.; Escalé, F.; Laso, M. *J. Comput. Chem.*, in press.
- (14) Metropolis, N.; Rosenbluth, A. W.; Rosenbluth, M. N.; Teller, A. H.; Teller, E. *J. Chem. Phys.* **1953**, 23, 1087.
- (15) Allen, M. P.; Tildesley, D. J. *Computer Simulation of Liquids*; Clarendon Press: Oxford, 1987.
- (16) Zanuy, D.; León, S.; Alemán, C.; Muñoz-Guerra, S. *Polymer* **2000**, 41, 4169.
- (17) León, S.; Navas, J. J.; Alemán, C. *Polymer* **1999**, 40, 7351.

MA001213B